respectively (mean value 10·1 e). The same value has been obtained for the Mg atom in MgF_2 (Niederauer & Göttlicher, 1970), in contrast with the 10·97 (3) e assigned to the Mg atom in dolomite, $CaMg(CO_3)_2$ (Effenberger, Kirfel & Will, 1983). We assume a quite ionic character to the Mg–O bond. The existence of a fully ionic bond in MgO has also been proposed from theoretical calculations (Causa, Dovesi, Pisani & Roetti, 1986).

The second feature refers to the electron bridge (M_O) of $\rho = 0{\cdot}24$ e Å^{-3} observed between O atoms (see lower part of Fig. 5) belonging to two different CO_3 groups. This maximum is repeated six times by the $\bar{3}$ site symmetry of the Mg atom, so forming a sectional ring cloud around it parallel to the *xy* plane. A similar electron bridge of 0·18 e Å^{-3} was also observed between neighbouring F^- anions in MgF_2 (Niederauer & Göttlicher, 1970). If we consider them as the result of a weak overlap of the lone pairs of the six O atoms surrounding the Mg atoms, we can explain (see Fig. 5) why they are located between O and O′ and not between O and O″.

Opposite a CO bond, overlapping of the lone-pair clouds is not observed. On O″ the angle between the CO bond and the line from O″ to the region where overlapping is expected is about 160° while all the other corresponding angles are between 85 and 125°. The distance between O atoms with overlapping is a little larger (3·02 Å between O and O′ and 2·93 Å between O and O″). We assume that the contact of the lone-pair clouds leads to a repulsive force between the O atoms. In $NaNO_3$, with lower charge in the cation, the O–O distances are larger (3·4 Å) and overlapping of the electron clouds is not observed.

It is desirable that further studies involving other experimental techniques confirm the existence of such O–O interactions.

We are indebted to the Deutsche Forschungsgemeinschaft and to the German and Spanish Governments for their financial support.

References

BURTON, B. & KIKUCHI, R. (1984). *Am. Mineral.* **69**, 165–175.

CAUSA, M., DOVESI, R., PISANI, C. & ROETTI, C. (1986). *Acta Cryst.* B**42**, 247–253.

EFFENBERGER, H., KIRFEL, A. & WILL, G. (1983). *Tschermaks Mineral. Petrogr. Mitt.* **31**, 151–164.

EFFENBERGER, H., MEREITER, K. & ZEMANN, J. (1981). *Z. Kristallogr.* **156**, 233–243.

GÖTTLICHER, S. (1968). *Acta Cryst.* B**24**, 122–129.

GÖTTLICHER, S. & KIESELBACH, B. (1976). *Acta Cryst.* A**32**, 185–192.

GÖTTLICHER, S. & KNÖCHEL, C. D. (1980). *Acta Cryst.* B**36**, 1271–1277.

HUMBERT, P. & PLIQUE, F. (1972). *C. R. Acad. Sci. Ser. B*, **275**, 391–394.

International Tables for X-ray Crystallography (1974). Vol. IV. Birmingham: Kynoch Press. (Present distributor Kluwer Academic Publishers, Dordrecht.)

MARKGRAF, S. A. & REDER, R. J. (1985). *Am. Mineral.* **70**, 590–600.

NIEDERAUER, K. & GÖTTLICHER, S. (1970). *Z. Angew. Phys.* **29**, 16–21.

OH, K. D., MORIKAWA, H., IWAI, S. & AOKI, H. (1973). *Am. Mineral.* **58**, 1029–1033.

PANKE, D. & WÖLFEL, E. (1969). *Z. Kristallogr.* **129**, 9–28.

PAULING, L. (1931). *J. Am. Chem. Soc.* **53**, 1367–1402.

PETERSON, R. G., ROSS, F. K., GIBBS, G. V., CHIARI, G., GUPTA, A. & TOSSELL, J. A. (1979). *Trans. Am. Geophys. Union*, **60**, 415.

SCHÄFER, C., MATOSI, F. & ADERHOLD, H. (1930). *Z. Phys.* **65**, 289–318.

VIDAL-VALAT, G., VIDAL, J. P. & KURKI-SUONIO, K. (1978). *Acta Cryst.* A**34**, 594–602.

WASER, J. (1955). *Acta Cryst.* **8**, 731.

ZACHARIASEN, W. H. (1967). *Acta Cryst.* **23**, 558–564.

ZEMANN, J. (1981). *Fortschr. Mineral.* **59**, 95–116.

ZOBETZ, E. (1982). *Z. Kristallogr.* **160**, 81–92.

Acta Cryst. (1988). B**44**, 367–373

Rietveld Profile Analysis of Calcined $AlPO_4$-11 Using Pulsed Neutron Powder Diffraction

BY JAMES W. RICHARDSON JR,* JOSEPH J. PLUTH AND JOSEPH V. SMITH

Department of Geophysical Sciences and Materials Research Laboratory, The University of Chicago, Chicago, Illinois 60637, *USA*

(*Received* 18 *August* 1987; *accepted* 15 *March* 1988)

Abstract

Aluminium phosphate, $AlPO_4$, $M_r = 121{\cdot}95$, orthorhombic, *Icmm* (disordered Al,P), *Icm*2 (ordered Al,P), $a = 13{\cdot}5333$ (8), $b = 18{\cdot}4845$ (10), $c = 8{\cdot}3703$ (4) Å, $V = 2094$ Å^3, $Z = 20$, $D_x = 1{\cdot}93$ g cm^{-3}, $T \simeq 295$ K, $R_{wp} = 0{\cdot}031$, $R_F^2 = 0{\cdot}109$ (*Icmm*) and $R_{wp} = 0{\cdot}027$, $R_F^2 = 0{\cdot}058$ (*Icm*2) for 1017 independent reflections. Sample calcined at 873 K and dehydrated at 573 K. Time-of-flight neutron powder diffraction data were

* Also Pulsed Neutron Source Division, Argonne National Laboratory, Argonne, Illinois 60439, USA.

0108-7681/88/040367-07$03.00

taken on the GPPD diffractometer at the Argonne National Laboratory Intense Pulsed Neutron Source. The structure was refined by Rietveld profile analysis in the range $d = 0{\cdot}86$–$3{\cdot}91$ Å in two space groups: *Icmm* assuming no ordering of Al and P, and *Icm*2 assuming strict alternation of Al and P on tetrahedral nodes. The $AlPO_4$-11 framework with $(4.6.10)_4(6.6.10)_1$ connectivity contains non-connecting, one-dimensional channels bounded by 6-rings, and spanned by elliptical 10-rings with free diameter $7{\cdot}0 \times 4{\cdot}1$ Å. Bond distance ranges and mean values are as follows: *Icmm*, (P,Al)–O 1·45–1·80, 1·60 (9) Å; *Icm*2, P–O 1·31–1·66, 1·51 (11) Å, Al–O 1·54–1·84, 1·68 (8) Å. Values in parentheses are standard deviations for averaging. (P,Al)–O–(P,Al) bond-angle ranges are 127–180° (*Icmm*) and 131–175° (*Icm*2). Although the *Icm*2 refinement appears to confirm the assumed P,Al ordering, it should be pointed out that the bond distance ranges are 2–3 times those found in a single-crystal X-ray refinement of as-synthesized MnAPO-11 with encapsulated diisopropylamine. In addition, a stable refinement of the non-centrosymmetric, strongly pseudo-symmetric structure was produced only after a refined model was obtained from the single-crystal experiment. Furthermore, it was important to remove a significant non-crystalline contribution to the total scattering. Caution is needed in the interpretation of Rietveld results for complex ordered structures, especially those which are non-centrosymmetric and lack supercell reflections.

Introduction

Some calcined members of a new series of synthetic aluminophosphates (Wilson, Lok & Flanigen, 1982; Wilson, Lok, Messina, Cannan & Flanigen, 1982, 1983) ($AlPO_4$-*n*) display important molecular-sieve properties and a range of structural properties. While $AlPO_4$-17, $AlPO_4$-20 and $AlPO_4$-24 are analogs of zeolites (erionite, sodalite and analcime, respectively) (Wilson *et al.* 1982, 1983; Pluth, Smith & Bennett, 1986), $AlPO_4$-5 displays a new structure type (Bennett, Cohen, Flanigen, Pluth & Smith, 1983) which is based on the theoretical four-connected three-dimensional net No. 81 (Smith, 1978), with non-connecting parallel one-dimensional channels spanned by 12-rings and having (4.6.12) connectivity. The cell dimensions of $AlPO_4$-11 are consistent with another new structure type obtained by removal of one set of 4-rings in the $AlPO_4$-5 net, corresponding to a σ^{-1} transformation (Shoemaker, Robson & Broussard, 1973) and resulting in an orthorhombic net with *Icmm* symmetry and $(4.6.10)_4(6.6.10)_1$ connectivity (Bennett & Smith, 1985). We have tested this proposed structure by Rietveld refinement of time-of-flight neutron diffraction powder data. A preliminary report has been given by Bennett, Richardson, Pluth & Smith (1987). The aim of this paper is to provide a more detailed account of the structure refinement together with an evaluation of the reliability of the structural data. Particularly important are the implications for neutron powder determination of complex frameworks with possible ordering of tetrahedral species.

Experimental

$AlPO_4$-11 was synthesized by hydrothermal crystallization of a reactive gel consisting of hydrated aluminium oxide, orthophosphoric acid and water, mixed with di-*n*-propylamine. The crystalline powder was calcined at 873 K overnight. The sample was transferred to a thin-walled vanadium can (1.1 cm diameter, 15·5 cm long) with a glass tube epoxied to its open end, heated to 573 K and evacuated using an Hg diffusion pump. The calcined sample was sealed at temperature by fusing the end of the glass tube and mounted in the General Purpose Powder Diffractometer on the Intense Pulsed Neutron Source (IPNS) at Argonne National Laboratory. Time-of-flight diffraction data were collected at 295 K with detectors positioned at fixed scattering angles $2\theta = \pm 150$, ± 90, ± 60, $+30$ and $-20°$ for approximately 20 h. Structural refinements were performed using data collected at $\pm 90°$.

The data were analyzed with the Rietveld refinement technique (Rietveld, 1969), modified for use with time-of-flight data from a pulsed neutron source (Jorgensen & Rotella, 1982; Von Dreele, Jorgensen & Windsor, 1982). The coherent neutron-scattering lengths (fm) were as follows: $b(\text{Al}) = 3.45$, $b(\text{P}) = 5.13$, $b(\text{O}) = 5.81$, $b(T = \text{Al,P disordered}) = 4.29$. The background was fitted with a refinable six-parameter analytical function (Rotella, 1986). The eight refinable peak-shape parameters of the resolution function (Carpenter *et al.*, 1975; Rotella, 1986) were determined previously from an Si powder pattern; however, the $AlPO_4$-11 Bragg peaks were broadened relative to the instrumental function and the Gaussian components of the resolution function were varied during the refinement.

Refinement

Starting atomic positions and lattice parameters for the Rietveld profile refinement were obtained from the theoretical net No. 263 of Bennett & Smith (1985). As the refinement proceeded, it became obvious that there was significant non-crystalline scattering, as evidenced by an additional slowly oscillating component superimposed on the Bragg pattern. As with the Rietveld refinement of $AlPO_4$-5 (Richardson, Pluth & Smith, 1987), Fourier filtering (Richardson & Faber, 1985) produced a fit to the non-crystalline scattering component. Fourier filtering involves Fourier transforma-

tion of the residual intensities (observed minus calculated) to produce a real-space correlation function related to an atomic radial distribution function (RDF). Reverse Fourier transformation of the correlation function (summing from $r = 0{\cdot}0$ to $15{\cdot}0$ Å) produced a smooth fit to the oscillatory component which was subtracted from the original data for continued refinement. Fourier filtering was performed iteratively, as previously described (Richardson & Faber, 1985). To facilitate the Fourier filtering, the Rietveld refinement program used in this analysis has been modified (Rotella, 1986) such that estimated standard deviations are based on the original intensities, regardless of the data being used in the actual refinement. All data in the full range of analysis were used; not just those data thought to be contributing to Bragg reflections.

Icmm

In this space group, the Al and P atoms are randomly distributed on the tetrahedral (T) sites. The asymmetric unit contains three types of T atoms and eight O atoms. The lattice parameters, conventional background parameters and positional parameters were refined to convergence (shift/e.s.d. $< 0{\cdot}3$), with the original, uncorrected data. A first approximation to the non-crystalline scattering component was calculated and subtracted from the original data using the Fourier-filtering procedure. Additional refinements, using the corrected data, included individual isotropic thermal parameters, the Gaussian components to the peak-shape function along with extinction and absorption parameters. No structural constraints were applied

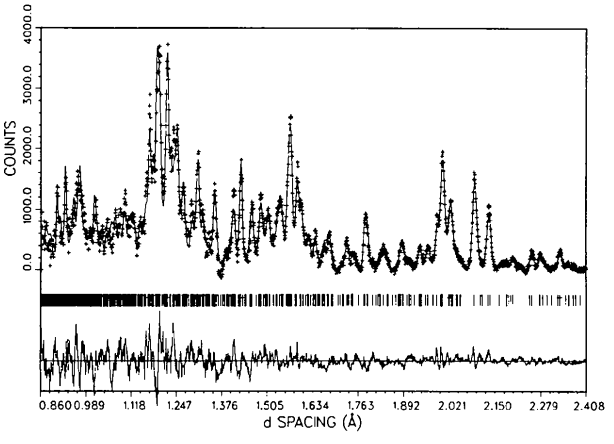

Fig. 1. Final profile plot from refinement of $AlPO_4$-11 in space group *Icmm*. The plus signs (+) are the raw data points and the solid line is the calculated profile. A difference curve is shown at the bottom of the diagram. Vertical bars below the profile indicate the positions of Bragg reflections for $AlPO_4$-11 included in the calculations. Vertical bars with horizontal cross bars indicate Bragg positions for Al. Calculated background and non-crystalline scattering contributions have been removed before plotting.

(Baerlocher, 1982), although occasional manual adjustments based on distance least-squares calculations (Baerlocher, Hepp & Meier, 1967) were made, with no improvement in the refinement.

The atomic displacement parameters of some of the O atoms in $AlPO_4$-11 were found to be very anisotropic from single-crystal X-ray refinements of the MnAPO-11 analog (Pluth, Smith & Richardson, 1988). Anisotropic Rietveld refinement of $AlPO_4$-11 in *Icmm* resulted in little improvement of the fit, even though a large number of parameters were added to the model, and the final cycles of the Rietveld refinement were completed using isotropic displacement parameters. A final Fourier-filtering calculation was made and the refinement again converged. F_o and $(F_o - F_c)$ Fourier maps revealed no additional information.

Relatively weak impurity lines with d-spacings near 2·33, 1·43, 1·22 Å, *etc.*, were attributable to scattering from the aluminium end cap ($Fm3m$, $a = 4{\cdot}0457$ Å), and were fitted as a second phase. The final profile fit based on the two-phase refinement is shown in Fig. 1.* The final structural parameters for $AlPO_4$-11 are provided in Tables 1–3.

Icm2

In this space group strict alternation of the Al and P atoms on the tetrahedral nodes, with consequent loss of mirror planes perpendicular to **c**, is assumed. The asymmetric unit contains three types of Al atoms, three P atoms and eleven O atoms. Rietveld refinement in this space group is very unstable as we learned from failures using theoretical models and models produced by distance least-squares fitting (Baerlocher *et al.*, 1967) and empirical methods. New starting positional parameters were obtained from the successful single-crystal X-ray refinement of MnAPO-11. Diffraction data resulting from the final Fourier-filtering correction for the *Icmm* refinement were used in subsequent refinements. Because some of the O atoms were known to be very anisotropic, separate isotropic and anisotropic refinements were made. Atom sites originally related by the mirror symmetry in *Icmm*, *e.g.*, P(1) and Al(1), O(5) and O(5′), were constrained to have equal displacement parameters. Once the displacement parameters were stabilized, positional parameters were varied, with displacement parameters fixed. Gradually all structural parameters were included in the refinements. A reasonably stable, but not strictly convergent, refinement was obtained for the anisotropic refinement, while the isotropic refinement quickly moved toward

* A list of numerical values corresponding to the data in Fig. 1 has been deposited with the British Library Document Supply Centre as Supplementary Publication No. SUP 44835 (9 pp.). Copies may be obtained through The Executive Secretary, International Union of Crystallography, 5 Abbey Square, Chester CH1 2HU, England.

Table 1. *Crystal data for* $AlPO_4$-11

	Icmm	*Icm2*
Space group		
a_0 (Å)	13·5333 (8)	13·5336 (7)
b_0 (Å)	18·4845 (10)	18·4821 (10)
c_0 (Å)	8·3703 (4)	8·3703 (4)
Range of data (Å)	0·86–3·91	0·86–3·91
No. of independent reflections	1017	1017
No. of variable parameters	48	113
R_{wp}* (%)	3·06	2·66
R_{F^2}† (%)	10·85	5·85

* $R_{wp} = 100\{\sum_i w_i[y(\text{obs.})-(1/c)y(\text{calc.})]^2/\sum_i w_i[y(\text{obs.})]^2\}^{1/2}$.
† $R_{F^2} = 100\sum_i\{\text{ABS}[I(\text{obs.})-I(\text{calc.})]\}/\sum_i\{\text{ABS}[I(\text{obs.})]\}$.

Table 2. *Atomic coordinates and displacement parameters* ($\times 10^3$) *for* $AlPO_4$-11 *in space group Icmm*

	Site	Symmetry	x	y	z	U_{iso}(Å^2)
$T(1)$	16(j)	1	0·1364 (7)	0·0270 (5)	0·1929 (11)	37 (3)
$T(2)$	16(j)	1	0·9535 (6)	0·1052 (6)	0·3135 (11)	50 (3)
$T(3)$	8(i)	m	0·8543 (9)	0·2500	0·1948 (13)	23 (3)
O(1)	8(h)	m	0·1431 (14)	0·0489 (10)	0·0000	139 (6)
O(2)	8(h)	m	0·9421 (10)	0·1125 (8)	0·5000	102 (4)
O(3)	4(e)	mm	0·8510 (14)	0·2500	0·0000	85 (5)
O(4)	8(g)	2	0·2500	0·0700 (5)	0·2500	78 (4)
O(5)	16(j)	1	0·0610 (6)	0·0906 (4)	0·2478 (10)	68 (3)
O(6)	16(j)	1	0·1176 (6)	0·9526 (5)	0·2381 (16)	91 (4)
O(7)	16(j)	1	0·9134 (8)	0·1768 (5)	0·2514 (18)	107 (4)
O(8)	4(d)	2/m	0·7500	0·2500	0·2500	69 (5)

Table 3. *Bond distances* (Å) *and angles* (°) *for* $AlPO_4$-11 *in space group Icmm*

$T(1)$–O(1)	1·67 (1)	$T(1)$–O(1)–$T(1)$	151 (1)
–O(4)	1·80 (1)	$T(2)$–O(2)–$T(2)$	165 (1)
–O(5)	1·62 (1)	$T(3)$–O(3)–$T(3)$	177 (3)
–O(6)	1·45 (1)	$T(1)$–O(4)–$T(1)$	127 (1)
⟨$T(1)$–O⟩	1·64	$T(1)$–O(5)–$T(2)$	144 (1)
		$T(1)$–O(6)–$T(2)$	149 (1)
		$T(2)$–O(7)–$T(3)$	172 (1)
$T(2)$–O(2)	1·57 (1)	$T(3)$–O(8)–$T(3)$	180
–O(5)	1·58 (1)		
–O(6)	1·57 (1)	O(1)–$T(1)$–O(4)	96 (1)
–O(7)	1·52 (1)	–O(5)	98 (1)
⟨$T(2)$–O⟩	1·56	–O(6)	120 (1)
		O(4)–$T(1)$–O(5)	98 (1)
		–O(6)	120 (1)
$T(3)$–O(3)	1·63 (1)	O(5)–$T(1)$–O(6)	119 (1)
–O(7)	1·64 (1)		
–O(7′)	1·64 (1)	O(2)–$T(2)$–O(5)	117 (1)
–O(8)	1·49 (1)	–O(6)	113 (1)
⟨$T(3)$–O⟩	1·60	–O(7)	103 (1)
		O(5)–$T(2)$–O(6)	108 (1)
		–O(7)	111 (1)
⟨T–O⟩	1·60	O(6)–$T(2)$–O(7)	104 (1)
		O(3)–$T(3)$–O(7)	108 (1)
		–O(7′)	108 (1)
		–O(8)	107 (1)
		O(7)–$T(3)$–O(7′)	111 (1)
		–O(8)	112 (1)
		O(7′)–$T(3)$–O(8)	112 (1)

the average *Icmm* structure. The final profile fit for the anisotropic refinement is given in Fig. 2 and structural parameters are given in Tables 4 and 5.

Discussion

Framework

The structure of $AlPO_4$-11 is composed of AlO_4 and PO_4 tetrahedra. Three vertices of each tetrahedron are linked to form sheets containing 4-, 6- and 10-rings. The three-dimensional framework (Fig. 3) is produced by linking the remaining vertices which project alternately up and down normal to these sheets. Columns of 4-, 6- and 10-rings are formed running parallel to **c**. Isolated parallel channels spanned by 10-rings have an elliptical cross section and have a surface bounded by 6-rings. The diameters of the major and minor axes are 9·6 and 6·7 Å, which result in a channel opening of 7·0 by 4·1 Å assuming a free diameter of 2·6 Å for O.

The framework structures of $AlPO_4$-11 and $AlPO_4$-5 are closely related (see Figs. 4 and 5). The sheets of $AlPO_4$-5 are composed of 4-, 6- and 12-rings. Removal of a pair of opposing 4-rings in $AlPO_4$-5 converts the 12-ring to a 10-ring and generates the sheet found in $AlPO_4$-11. Whereas 4- and 6-rings alternate around the 12-ring channel of $AlPO_4$-5, two pairs of 6-rings are adjacent around the 10-ring channel of $AlPO_4$-11. When the σ^{-1} transformation is performed, therefore, O(4) atoms of $AlPO_4$-5 related by twofold symmetry are superimposed into O(8) of $AlPO_4$-11. Because O(8) is confined to a mirror plane by the *Icmm* (and *Icm*2) symmetry of $AlPO_4$-11, the observed distortions of the 6-rings of $AlPO_4$-11 relative to $AlPO_4$-5 may be expected.

Refinement

The precision of the Rietveld refinement of $AlPO_4$-11 is not as high as that for a single-crystal determination of MnAPO-11 (Pluth *et al.*, 1988), or for that matter, the Rietveld refinement of $AlPO_4$-5. For the disordered model of $AlPO_4$-11, T–O distances range from 1·45 (1) to 1·80 (1) Å, and T–O–T angles from 127 (1) to 180°. Respective ranges for the Rietveld refinement of the disordered model of $AlPO_4$-5 were: 1·560 (6)–1·633 (9) Å and 146·6 (8)–176·1 (14)°. In addition, it is clear from the discrepancies in the profile fit (Fig. 1), particularly in the lower d-spacing range, that the disordered model is not completely representative of the

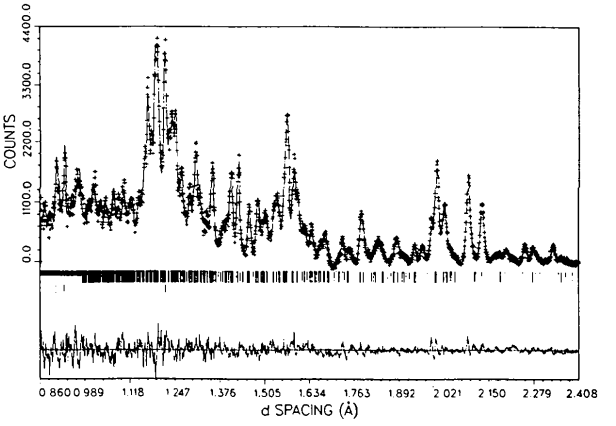

Fig. 2. Final profile plot from the *Icm*2 refinement of $AlPO_4$-11. Definitions are as in Fig. 1.

Table 4. *Atomic coordinates and displacement parameters* ($\times 10^3$) *for* $AlPO_4$-11 *in space group Icm2*

	Site	Symmetry	x	y	z	U_{iso}(Å^2)
P(1)	8(*c*)	1	0·143 (2)	0·025 (1)	0·182 (6)	35 (9)
Al(1)	8(*c*)	1	0·134 (2)	0·035 (2)	−0·199 (8)	35 (9)
P(2)	8(*c*)	1	0·953 (2)	0·104 (2)	−0·306 (5)	45 (9)
Al(2)	8(*c*)	1	0·949 (4)	0·102 (3)	0·317 (6)	45 (9)
P(3)	4(*b*)	*m*	0·857 (2)	0·250	0·185 (5)	24 (11)
Al(3)	4(*b*)	*m*	0·850 (4)	0·250	−0·185 (6)	24 (11)
O(1)	8(*c*)	1	0·143 (3)	0·039 (1)	0·000	154 (19)
O(2)	8(*c*)	1	0·945 (1)	0·105 (1)	0·517 (5)	77 (9)
O(3)	4(*b*)	*m*	0·860 (3)	0·250	0·024 (9)	123 (32)
O(4)	8(*c*)	1	0·242 (2)	0·068 (1)	0·243 (5)	64 (14)
O(5)	8(*c*)	1	0·068 (1)	0·088 (2)	0·252 (6)	68 (8)
O(5′)	8(*c*)	1	0·057 (1)	0·091 (2)	−0·257 (5)	68 (8)
O(6)	8(*c*)	1	0·118 (3)	0·955 (3)	0·232 (9)	108 (14)
O(6′)	8(*c*)	1	0·125 (3)	0·954 (3)	−0·264 (9)	108 (14)
O(7)	8(*c*)	1	0·913 (3)	0·179 (2)	0·232 (6)	111 (11)
O(7′)	8(*c*)	1	0·909 (3)	0·177 (2)	−0·263 (7)	111 (11)
O(8)	4(*b*)	*m*	0·762 (3)	0·250	0·234 (8)	89 (23)

Table 5. *Bond distances* (Å) *and angles* (°) *for* $AlPO_4$-11 *in space group Icm2*

P(1)–O(1)	1·57 (5)	Al(1)–O(1)	1·64 (6)
–O(4)	1·66 (3)	–O(4)	1·84 (4)
O(5)	1·64 (4)	O(5′)	1·58 (5)
–O(6)	1·39 (5)	–O(6′)	1·60 (5)
⟨P(1)–O⟩	1·57	⟨Al(1)–O⟩	1·67
P(2)–O(2)	1·50 (4)	Al(2)–O(2)	1·68 (4)
–O(5′)	1·48 (3)	–O(5)	1·74 (6)
–O(6′)	1·56 (6)	–O(6)	1·54 (6)
–O(7′)	1·52 (4)	–O(7)	1·67 (6)
⟨P(2)–O⟩	1·52	⟨Al(2)–O⟩	1·66
P(3)–O(3)	1·31 (6)	Al(3)–O(3)	1·80 (7)
–O(7)	1·57 (4) (×2)	–O(7′)	1·69 (4) (×2)
–O(8)	1·35 (4)	–O(8)	1·63 (5)
⟨P(3)–O⟩	1·45	⟨Al(3)–O⟩	1·70
⟨P–O⟩	1·51	⟨Al–O⟩	1·68
Distances across channel			
O(4)–O(4)	6·73	O(7)–O(7′)	9·55
O(5)–O(5′)	7·81		

P(1)–O(1)–Al(1)	167 (2)	P(1)–O(6)–Al(2)	152 (6)
P(2)–O(2)–Al(2)	174 (2)	P(2)–O(6′)–Al(1)	140 (3)
P(3)–O(3)–Al(3)	172 (4)	P(3)–O(7)–Al(2)	166 (4)
P(1)–O(4)–Al(1)	131 (2)	P(2)–O(7′)–Al(3)	168 (4)
P(1)–O(5)–Al(2)	140 (3)	P(3)–O(8)–Al(3)	175 (4)
P(2)–O(5′)–Al(1)	147 (3)		

structure of calcined $AlPO_4$-11. Irrespective of the details of the refinement, however, the proposed framework topology of $AlPO_4$-11 would probably be assumed to be correct from the Rietveld analysis. Fortunately, any residual doubt is removed by the single-crystal refinement of the MnAPO analog.

As to the question of the P and Al ordering, the isotropic and anisotropic refinements gave rather different results, with the isotropic refinement indicating greater disorder. Ranges and mean values of bond distances are: isotropic, P–O 1·47 (3)–1·67 (4), 1·56 Å, Al–O 1·50 (9)–1·80 (4), 1·63 Å; anisotropic, P–O 1·31 (6)–1·66 (3), 1·51 Å, Al–O 1·54 (6)–1·84 (4), 1·68 Å. Mean distances expected for complete ordering are P–O = 1·46–1·48 Å and Al–O = 1·70–1·71 Å. (A riding-motion correction of 0·04–0·05 Å would increase the mean distances to the expected values of approximately 1·54 and 1·74 Å). The anisotropic refinement gave a noticably better fit to the observed diffraction profile ($R_F^2 = 5{\cdot}8\%$ as compared with $R_F^2 = 12{\cdot}6\%$), and produced reasonable anisotropic displacements, although some atoms had sufficiently small β_{33}'s to become non-positive definite. However, neither refinement was strictly convergent, and the refinements by themselves do not prove without a doubt that the ordering is complete.

The recently reported Rietveld refinement, from X-ray data, of $AlPO_4$-12 TAMU (Rudolf, Saldarriage-Molina & Clearfield, 1986), which is based on the

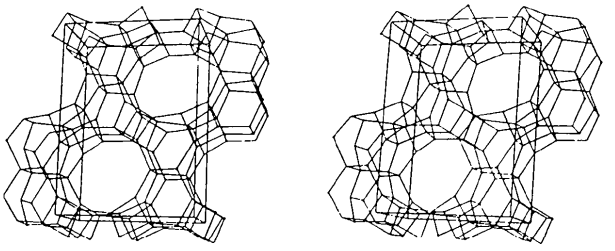

Fig. 3. Stereoview of the $AlPO_4$-11 unit cell, showing the three-dimensional net produced by connecting the tetrahedral nodes. Strict alternation of Al and P is assumed.

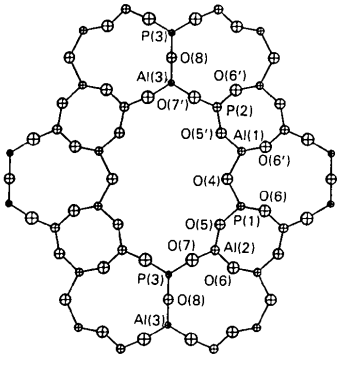

Fig. 4. *ORTEP* (Johnson, 1965) drawing of $AlPO_4$-11 projected along [001]. Atoms O(1), O(2) and O(3) are not shown, and would be projected onto *T* atoms.

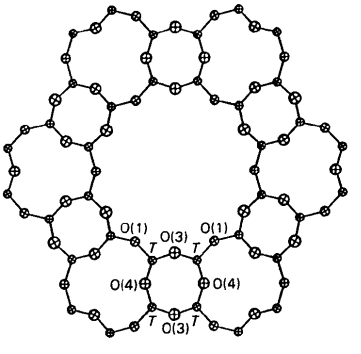

Fig. 5. *ORTEP* drawing of $AlPO_4$-5 projected along [001]. Atom O(2) is not shown. Note the orientation of atom O(4) relative to that of O(8) in Fig. 4.

theoretical net No. 102 (Smith, 1979), produced an ordered framework with significantly narrower ranges of distances [P–O = 1·481–1·615, mean value = 1·556 (15) Å and Al–O = 1·702–1·822, mean value = 1·768 (13) Å] than those found in the refinements of $AlPO_4$-11. [Note that $AlPO_4$-12 TAMU has the same structure as $AlPO_4$-33 (Patton & Gajek, 1984); manuscript in preparation]. There are two significant factors which contribute to this. First, the ordering of P and Al in $AlPO_4$-12 TAMU results in a doubling of the unit cell and thus the introduction of additional superlattice reflections. Because space groups *Icmm* and *Icm*2 have the same set of reflections, the ordered refinement of $AlPO_4$-11 relies strictly on intensities. Secondly, although the space groups for $AlPO_4$-12 TAMU ($P2_12_12$) and $AlPO_4$-11 (*Icm*2) are both non-centrosymmetric, the phases of some reflections for $P2_12_12$, as well as the origin, are fixed by symmetry. For *Icm*2, all reflections can have any phase ranging from 0 to 2π, and the origin is fixed by arbitrarily fixing the z coordinate for a single atom.

Non-crystalline component

For the purposes of these refinements Fourier filtering was used merely as a way to remove undesirable background intensities. The Fourier filtering is capable, however, of providing reasonably accurate information about the source of the non-crystalline scattering, in the form of interatomic correlation distances. In order to obtain accurate real-space non-crystalline correlation information, data to $d = 0{\cdot}50$ Å or lower are needed. The quality of our crystalline data does not justify refinement so deep into reciprocal space. We have, however, used the residual differences down to $d = 0{\cdot}45$ Å (without further refinement) to produce approximate interatomic distances. Resulting distances of 1·57, 2·55, 2·97, 4·19 and 5·13 Å can be attributed to T–O, O–O, T–T' (1st neighbor), T–T'' (2nd neighbor, 4-ring) and T–T'' (2nd neighbor, 6-ring) interactions. These distances are consistent with average angles of O–T–O = 109°, T–O–T' = 142°, T–T'–T'' (4-ring) = 90° and T–T'–T'' (6-ring) = 119°. These values are all close to those actually found in crystalline $AlPO_4$-11, indicating that the oscillatory interference pattern superimposed on the Bragg scattering results from material having an atomic arrangement similar to that of $AlPO_4$-11, but lacking the long-range periodicity.

Concluding remarks

The Rietveld refinement results when taken at face value tend to be falsely optimistic. The scatter in structural parameters such as bond distances is larger than the estimated errors would suggest. On the whole, however, the Rietveld profile refinement technique has produced a reasonable refinement of this complex structure. In addition, we have demonstrated, with the use of Fourier filtering, that significant contributions from non-crystalline components can be effectively removed and tentatively identified. The extremely broad diffraction peaks observed for $AlPO_4$-11 prevent us from taking full advantage of the resolution capabilities of the instrumentation, even though the Rietveld technique, which involves refinement based on profile intensities rather than integrated intensities, is designed to accommodate overlapping peaks.

We thank NSF for CHE 84-05167 and for general support for the Materials Research Laboratory (DMR 82-16892). E. M. Flanigen, S. T. Wilson and R. L. Patton kindly supplied the crystals and discussed the results. J. M. Bennett informed JVS about the identity of the structures of $AlPO_4$-33 and $AlPO_4$-12 TAMU after completion of this work. JWR acknowledges J. Faber Jr and R. L. Hitterman for assistance in the use of their instrument and financial support by the US Department of Energy under contract W-31-109-ENG-38.

References

BAERLOCHER, C. (1982). *The X-ray Rietveld System.* Institut fuer Kristallographie und Petrographie, ETH, Zurich, Switzerland.

BAERLOCHER, C., HEPP, A. & MEIER, W. M. (1967). *A Program for the Simulation of Crystal Structures by Geometric Refinement.* Institut fuer Kristallographie und Petrographie, ETH, Zurich, Switzerland.

BENNETT, J. M., COHEN, J. P., FLANIGEN, E. M., PLUTH, J. J. & SMITH, J. V. (1983). *Am. Chem. Soc. Symp. Ser.* **218**, 109–118.

BENNETT, J. M., RICHARDSON, J. W. JR, PLUTH, J. J. & SMITH, J. V. (1987). *Zeolites*, **7**, 160–162.

BENNETT, J. M. & SMITH, J. V. (1985). *Z. Kristallogr.* **171**, 65–68.

CARPENTER, J. M., MUELLER, M. H., BEYERLEIN, R. A., WORLTON, T. G., JORGENSEN, J. D., BRUN, T. O., SKOLD, K., PELIZZARI, C. A., PETERSON, S. W., WATANABE, N., KIMURA, M. & GUNNING, J. E. (1975). *Proc. Neutron Diffraction Conf., Petten, August* 5–6, RCN-234, pp. 192–208. Reactor Centrum Nederland, Petten, The Netherlands.

JOHNSON, C. K. (1965). *ORTEP.* Report ORNL-3794. Oak Ridge National Laboratory, Tennessee, USA.

JORGENSEN, J. D. & ROTELLA, F. J. (1982). *J. Appl. Cryst.* **15**, 27–34.

PATTON, R. L. & GAJEK, R. T. (1984). US Patent 4 473 663.

PLUTH, J. J., SMITH, J. V. & BENNETT, J. M. (1986). *Acta Cryst.* C**42**, 283–286.

PLUTH, J. J., SMITH, J. V. & RICHARDSON, J. W. JR (1988). *J. Phys. Chem.* Submitted.

RICHARDSON, J. W. JR & FABER, J. JR (1985). *Advances in X-ray Analysis*, Vol. 29, pp. 143–152. New York: Plenum Press.

RICHARDSON, J. W. JR, PLUTH, J. J. & SMITH, J. V. (1987). *Acta Cryst.* C**43**, 1469–1472.

RIETVELD, H. M. (1969). *J. Appl. Cryst.* **2**, 65–71.

ROTELLA, F. J. (1986). *Users Manual for Rietveld Analysis of Time-of-Flight Neutron Powder Diffraction Data at IPNS.* Argonne National Laboratory, Illinois, USA.

RUDOLF, P. R., SALDARRIAGE-MOLINA, C. & CLEARFIELD, A. (1986). *J. Phys. Chem.* **90**, 6122–6125.

SHOEMAKER, D. P., ROBSON, M. E. & BROUSSARD, L. (1973). *Molecular Sieves*, edited by J. B. VYTTERHOVEN, p. 138. Leuven Univ. Press.
SMITH, J. V. (1978). *Am. Mineral.* **63**, 960–969.
SMITH, J. V. (1979). *Am. Mineral.* **64**, 551–562.
VON DREELE, R. B., JORGENSEN, J. D. & WINDSOR, C. G. (1982). *J. Appl. Cryst.* **15**, 581–589.
WILSON, S. T., LOK, B. M. & FLANIGEN, E. M. (1982). US Patent 4 310 440.
WILSON, S. T., LOK, B. M., MESSINA, C. A., CANNAN, T. R. & FLANIGEN, E. M. (1982). *J. Am. Chem. Soc.* **104**, 1146–1167.
WILSON, S. T., LOK, B. M., MESSINA, C. A., CANNAN, T. R. & FLANIGEN, E. M. (1983). *Am. Chem. Soc. Symp. Ser.* **218**, 79–106.

Acta Cryst. (1988). B**44**, 373–377

Structure of Sapphirine: its Relation to the Spinel, Clinopyroxene and β-Gallia Structures

BY J. BARBIER

Department of Chemistry, McMaster University, Hamilton, Ontario L8S 4M1, Canada

AND B. G. HYDE

Research School of Chemistry, Australian National University, GPO Box 4, Canberra, ACT 2601, Australia

(*Received* 23 *December* 1987; *accepted* 24 *March* 1988)

Abstract

A new description of the sapphirine structure is proposed in which it is shown to result from the regular intergrowth at the unit-cell level of slabs of the spinel and clinopyroxene structures. The latter structure is also shown to be simply related to the β-gallia structure by a periodic slip operation. These two structural relations appear to be directly relevant to the complex crystal chemistry of sapphirine.

1. Introduction

Sapphirine with the ideal composition $Mg_4Al_8Si_2O_{20}$ is an uncommon mineral, the crystal structure of which remained unsolved for a long time. Moore (1968, 1969) carried out the first structure determination for the monoclinic form (sapphirine-2M) while, more recently, Merlino (1980) determined the structure of the triclinic form (sapphirine-1Tc). Both polymorphs have cubic close-packed O atoms and their X-ray diffraction spectra show strong similarities to that of spinel, but no simple relationship could be established between the sapphirine and spinel structures. For instance, Moore (1969) referred to the topology of sapphirine as being 'quite distinct' from that of spinel.

The recent identification of a new sapphirine-like phase, $Mg_4Ga_8Ge_2O_{20}$ (Barbier, 1988), led us to re-examine this structure type in terms of its possible relationship to spinel.* This resulted in a new description of the sapphirine structure which is presented here and which is based on the intergrowth at the unit-cell level of spinel/β-gallia or spinel/pyroxene structural elements.

2. The sapphirine structure

Chemical analyses of natural and synthetic sapphirines commonly yield compositions slightly enriched in aluminium *via* the substitution reaction $2Al = Mg + Si$ (*e.g.* Higgins, Ribbe & Herd, 1979; Bishop & Newton, 1975). Nevertheless, the ideal stoichiometry $Mg_4Al_8Si_2O_{20}$ will be used here for simplicity and also because it directly results from the building principle of the sapphirine structure (see below).

The structure of sapphirine-2M [$P2_1/a$, $a = 11{\cdot}266$, $b = 14{\cdot}401$, $c = 9{\cdot}929$ Å, $\beta = 125{\cdot}46°$, $Z = 4$ (Moore, 1969)] is shown in Fig. 1 projected along the **a*** direction. It is based on an approximate cubic close packing of O atoms with (Mg, Al) and (Al, Si) atoms in octahedral and tetrahedral coordination, respectively. Owing to the difficulty of visualizing the sapphirine structure as a whole (*i.e.*, there is no short projection axis), its description by Moore (1969) and Merlino (1980) merely emphasized various structural elements within the {100} planes, such as walls of edge-sharing octahedra running parallel to **c**, separated by 'winged' pyroxene-like tetrahedral chains in the **b** direction and by isolated octahedra in the **a** direction.

Previous studies of sapphirine polymorphism (Merlino, 1973, 1980; Dornberger-Schiff & Merlino, 1974) also recognized that the structures of the monoclinic and triclinic forms are the end members of an order–disorder series corresponding to different stacking sequences of equivalent {010} layers. The width of

* Two other spinel-related compounds, $Mg_3Ga_2GeO_8$ (Barbier & Hyde, 1986) and $Mg_7Ga_2GeO_{12}$ (Barbier & Hyde, 1987), have previously been identified in the MgO–Ga_2O_3–GeO_2 system.

0108-7681/88/040373-05$03.00